Quantum electron transport through narrow constrictions in semiconductor nanostructures

Song He* and S. Das Sarma
Department of Physics, University of Maryland, College Park, Maryland 20742
(Received 13 November 1992; revised manuscript received 3 May 1993)

Detailed numerical results, with emphasis on the role of disorder and constriction geometry, are presented for the calculated conductance of quantum point contacts between high-mobility two-dimensional electron systems fabricated on semiconductor nanostructures. The conductance is calculated from the two-terminal multichannel transmission matrix formalism using the recursive single-particle Green's-function technique. The Green's functions are obtained recursively for a tight-binding two-dimensional disordered Anderson lattice model representing the constriction. The conductance is calculated as a function of the shape and the size of the constriction (i.e., its geometry) and the elastic disorder in the system.

The discovery,[1,2] in 1988, by two different experimental groups of the (approximate) ballistic conductance quantization phenomenon in narrow constrictions or quantum point contacts (in this paper, we use these two terms interchangeably, uncritically taking it for granted that, at least from the theorists' viewpoint, these represent the same structure) in GaAs microstructures created a flurry of activity which continues unabated. The original experimental results were interpreted on the basis of a simple one-dimensional model of the constriction where the density of states is inversely proportional to the electron velocity, and, therefore, the one-dimensional conductance $\mathcal{G}$ is trivially quantized. An alternative equivalent description, which has been much emphasized[3] in the recent theoretical literature on the subject, is to use the so-called two-terminal multichannel Landauer formula

$$g = \mathrm{Tr}(tt^{\dagger}) ,$$

where t is the transmission matrix through the constriction and $g = \mathcal{G}/(2e^2/h)$ is the dimensionless conductance. In the absence of any scattering (i.e., in the perfectly ballistic limit) the transmission matrix for the occupied one-dimensional subbands is trivially given by

$$t_{ij} = \delta_{ij} ,$$

where i,j are subband indices and δ_{ij} is the Kronecker δ function. (For the unoccupied subband, obviously $t_{ij} = 0$.) Combining the above we get the conductance quantization condition $g = n$. This derivation of the conductance quantization phenomenon, while not being manifestly wrong, is clearly inadequate or even irrelevant for the real point contacts or the constrictions. The above derivation uncritically assumes infinitely long, perfectly one-dimensional systems which are at $T = 0$ with no elastic or inelastic scattering in them whatsoever. In reality, the point contacts are very far from perfect one-dimensional channels. The constrictions usually have widths which are often larger than their lengths. Also, finite temperature effects and corrections arising from elastic scattering by impurity disorder (which could be small, but not zero) and from inelastic scattering (e.g., phonons) need to be taken into account. Thus, any nontrivial theory of conductance quantization phenomenon must incorporate the following aspects into the model: (1) the shape and finite size (i.e., the geometry) of the constriction; (2) elastic-scattering effects arising from finite disorder in real systems; and (3) finite temperature effects which tend to smear the sharp subband structure by thermal broadening. Inclusion of these issues clearly requires a model going well beyond the simplistic derivations outlined above.

In this paper, we present numerical calculations for the conductance of a quantum constriction with emphasis on the roles of the constriction geometry and elastic-scattering strength in the system. Our calculation is a model calculation where geometry and elastic scattering are parametrized by suitable (and, presumably realistic) parameters rather than being calculated microscopically from the detailed electronic properties of the constrictions themselves. In any case, at the present time our knowledge of the detailed microscopic electronic and structural properties of these constrictions is quite limited so that almost all theoretical treatments of the subject are forced to resort to some level of parametrization.

We use a two-dimensional nearest-neighbor tight-binding square lattice Anderson model to describe the quantum point contact. The quantum point contacts are usually made by nanolithographic fabrication of modulation-doped high-mobility two-dimensional electron-gas systems, and, therefore, a two-dimensional Anderson model is a reasonable starting point in this problem. In our idealized model for quantum constriction, we envision the constriction or the point contact to be connected to the outside reservoirs, the left and the right reservoirs, by ideal (i.e., coherent and ballistic, with neither elastic nor inelastic scattering allowed in the leads) connecting wires or leads. The constriction itself is of finite size and has a well-defined shape which is to be modeled by various geometries described later in this paper. The various pieces of the Hamiltonian are all treated within the nearest-neighbor hopping approximation. The voltage is measured as the electrochemical potential

0163-1829/93/48(7)/4629(7)/$06.00

difference between the reservoirs where the electrons are assumed to thermalize (i.e., come to equilibrium) via inelastic scattering. For this model, the conductance formula $g = \mathrm{Tr}(tt^{\dagger})$ applies[4] which we use uncritically in all our calculations in this paper. We note that one could use alternative models for studying the conductance quantization phenomenon, but the results would be qualitatively similar. There have been several calculations[5,6] of the conductance quantization phenomenon using a conductance formula essentially equivalent to ours.

We calculate the transmission matrix t for the constriction using the single-particle Green's function for the system which we obtain recursively. To obtain the Green's-function matrix elements defining the transmission matrix t needed for the calculation of the conductance $g \equiv \mathrm{Tr}(tt^{\dagger})$, we use the recursive technique which is well suited for our model nearest-neighbor hopping Hamiltonian. The basic idea of the recursive Green's-function method[4] is to construct the matrix elements of the Green's function in the entire Hilbert space by starting from those in some selected subspace. One builds up the Green's-function matrix elements in the entire Hilbert space in a recursive step-by-step manner by utilizing the hopping matrix elements of the Hamiltonian. We use the hopping energy and the lattice size as the unit of energy and the unit of length, respectively, in our calculations. Disorder and constriction geometry enter into our calculation through the diagonal term V_{lm} in our tight-binding Anderson model as explained below.

The recursive Green's-function calculation is standard[4-6] and details can be found in the literature. It has been used extensively in localization and other related studies in low-dimensional systems. The Green's function is built up recursively along the x direction one column at a time, starting from the left and using our model Hamiltonian. Once the relevant matrix elements of the Green's function are computed, the system conductance is calculated using $g \equiv \mathrm{Tr}(tt^{\dagger})$.

While we refer to the existing literature for the details of the recursive Green's-function computation, we explain below how we include various physical effects (e.g., disorder, shape, and size, i.e., the geometry of the constriction, finite temperature, and finite magnetic field) in our calculation of the constriction conductance.

(i) *Disorder.* In our model, the constriction region is disordered while the left and the right leads are perfectly ordered. Disorder is introduced through the site diagonal energies V_{lm} in the model Hamiltonian, a part of which is assumed to be random. We model the random disorder by taking the site energy V_{lm} to be randomly distributed uniformly (i.e., a square distribution) between energies $\pm W$. Thus, W, the half-width of the uniform distribution, becomes a measure of the strength of random disorder in our model. For $W=0$, the constriction itself becomes perfectly ballistic whereas for large W ($\gtrsim 1$) the system is highly disordered.

(ii) *Geometry.* The geometry of a particular constriction is also modeled by the site energies V_{lm} in our calculation. One can define the constriction geometry by, for example, defining V_{lm} to be very large in magnitude outside the boundary of the constriction and zero (except for the random disorder part) inside the constriction. This will make the electron wave function vanishingly small outside the boundary, effectively defining the constriction geometry. Thus, we write $V_{lm} = V_{lm}^{(1)} + V_{lm}^{(2)}$ where $V_{lm}^{(1)}$ is the random part arising from disorder as discussed above (i.e., $|V_{lm}^{(1)}| < W$) and $|V_{lm}^{(2)}|$ is effectively infinite outside the boundary of the constriction and is zero inside.

We have considered (Fig. 1) three distinct types of constriction geometries: Strip, wide-narrow-wide, and tapered. Within the tapered geometry, we consider three different structures (Fig. 1)—one where the constriction boundary is triangular in shape and in the other two, it is rounded. The strip geometry, which is a uniform quasi-one-dimensional structure, is the simplest, because here the constriction and the leads are identical with the same lateral size M. The length of the constriction L is entirely defined by the length of the disordered region, because other than disorder there is no difference between the leads and the constriction in this geometry. The wide-narrow-wide (WNW) structure has, as the name suggests, an abrupt nonadiabatic shape where a narrow constriction of length L and width M_c is interposed between infinitely long perfect leads of widths M ($>M_c$) each.

It is obvious that the strip and the WNW structures, both of which have been extensively studied in the literature, are two extreme idealizations (absolutely adiabatic and absolutely abrupt, respectively) of real constrictions whose geometry must lie somewhere in between these extreme shapes. (Neither the strip nor the WNW geometry has much physical relevance.) To model these intermediate structures, we consider constriction geometries (Fig. 1) with triangular and curved shapes. We can generate these various geometries by defining the shape of the constriction geometry to have the following parametric form:

$$y = x^{\alpha},$$

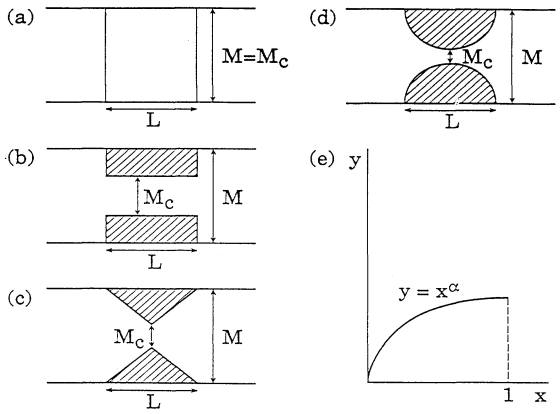

FIG. 1. This figure shows schematically the various constriction geometries used in our calculations: (a) Strip geometry, (b) wide-narrow-wide geometry, (c) adiabatic triangular geometry, and (d) adiabatic rounded (parabolic with $\alpha=0.5$, or quartic with $\alpha=0.25$) geometry. In (e) we show the parametric shape $y=x^{\alpha}$ used to model various constrictions with $\alpha=\infty$ (a); 0 (b); 1 (c); 0.25 and 0.50 (d).

where α (≥ 0) is the shape parameter that defines the constriction geometry (we also assume that the constriction is symmetric about its geometric center so that defining the shape only in one quadrant automatically defines the whole constriction). Note that $\alpha=0$ defines the WNW geometry where the width M_c (along the y direction) is constant throughout the constriction (and, is, therefore, independent of the x position along its length). On the other hand, the strip geometry may be thought of as having $\alpha \rightarrow \infty$. We have also considered constrictions with triangular ($\alpha=1$) and rounded ($\alpha=0.5$ and 0.25) shapes. In general, higher α implies that the constriction is more adiabatic. The width of the constriction is defined to be M_c, which is the width at the narrowest point of the constriction, or, equivalently the shortest lateral distance between the two boundaries. (In a WNW structure, M_c is constant throughout the constriction.) Note that the tapered constrictions can be thought of as adiabatic WNW structures, where the width of the system changes gradually (instead of abruptly as in a sharp WNW structure) from M to M_c and then back to M again over the whole length L of the constriction.

The geometry of the constriction is thus defined by L, M, M_c, and α, with L being the constriction length and M_c the constriction width (in the strip geometry $M=M_c$, whereas in the tapered geometry $M_c<M$ is the width at the narrowest point).

(iii) *Temperature.* The effect of finite temperature is introduced through the finite temperature Fermi distribution function $f(E)$ by writing

$$\mathcal{G}(T)=\int dE \left[-\frac{\partial f}{\partial E}\right] \mathcal{G}(T=0) ,$$

where $\mathcal{G}(T=0)$ is the conductance (defined earlier) at zero temperature which is calculated by our recursive Green's-function calculation and the Fermi distribution function is

$$f(E)=[1+e^{(E-\mu)/k_B T}]^{-1} ,$$

where μ is the chemical potential. While at $T=0$, only the conductance at the Fermi energy $\mu=E_F$ contributes, i.e., $\mathcal{G}(T=0)\equiv\mathcal{G}(E=E_F)$, and the finite temperature conductance is a convolution of contributions around the Fermi energy, depending on the magnitude of the thermal broadening.

(iv) *Finite magnetic field.* A finite magnetic field applied perpendicularly to the plane of constriction is included in some of our calculations by taking into account the magnetic-flux-dependent phase factors explicitly in the Green's function. Thus, we include the effect of the magnetic field in our calculations through the Peierls substitution. Since there is an underlying lattice in our calculations, our numerical results are periodic functions of the applied magnetic field. The magnetic field is applied only in the constriction part of the sample.

Next, we present our numerical results for the calculated two-terminal dimensionless conductance g of the constriction where $g=\mathcal{G}/(2e^2/h)=\mathrm{Tr}(tt^{\dagger})$, and we calculate the trace over the transmission matrix using the recursive Green's-function technique as described earlier in this section.

Our interest in this paper is in understanding in quantitative detail the conductance quantization phenomenon in the presence of various realistic physical constraints (e.g., disorder, temperature, finite size, and nonideal shape, etc.) one expects in real samples. As such, we show our computed g as a function of the Fermi energy (E_F) for different values of disorder (W), temperature (T), system size, and shape (L, M, M_c, and α). Since the unit of energy in our results is the hopping energy, the bandwidth of the two-dimensional Anderson model is 8 in our units. We show results covering only half of the bandwidth (i.e., for $-4\leq E_F\leq 0$) because the problem is symmetric around $E_F=0$. The unit of length is the lattice spacing throughout this paper. We concentrate mostly on disorder effects and on tapered geometries [Figs. 1(c)–1(e)] in this paper because the perfectly ordered strip and WNW structures have been extensively studied[3,5,6] in the literature.

In Fig. 2 we show our calculated $T=0$ conductance in the WNW geometry with $L=16$, $M=16$, $M_c=4$, and for $W=0$ (a), 0.05 (b), 0.20 (c), 1.60 (d). In the abrupt WNW geometry, as has been noted by many authors,[3,5] the quantization is not perfect even for $W=0$ because of the presence of sharp quantum resonances on the conductance plateaus which are clearly visible in Fig. 2. These resonances are associated with the reflection of the incident electron wave from the sharp corners of the WNW geometry (the resonance structure is not present in the

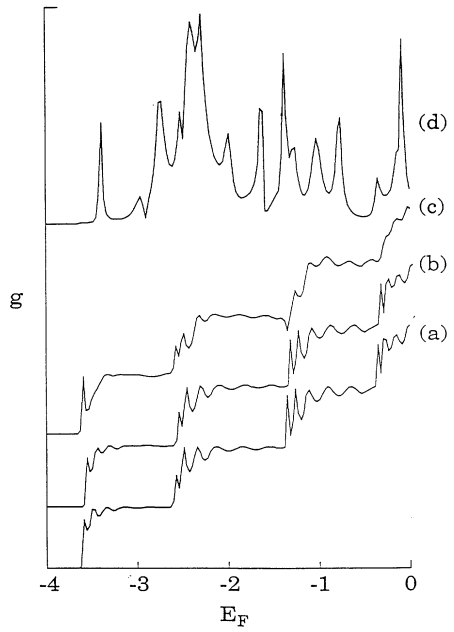

FIG. 2. The effect of the on-site impurity potential on the conductance of a quasi-one-dimensional structure in the wide-narrow-wide geometry. The widths of the wide and narrow regions are $M=16$ and $M_c=4$, respectively. The length of the narrow region is $L=16$. The strength of the impurity potential is $W=0.0$ (a), $W=0.05$ (b), $W=0.20$ (c), and $W=1.60$ (d).

perfectly adiabatic strip geometry results). The maxima of the oscillatory resonance structure on each of the conductance plateaus can be seen to reach the quantized $g=n$ value while most of the plateau is below the quantized conductance, and this result can be easily explained theoretically. But even this approximate quantization (with the maxima of the oscillatory resonance reaching up to $g=n$) is destroyed in the presence of disorder, and for large W the regular resonances disappear, leading to the conductance fluctuation[7] behavior. In Fig. 3 we show some further details of the conductance quantization phenomena for the WNW geometry. In Fig. 3 we show the calculated conductance g at $T=0$ for the WNW geometry for fixed $M_c=4$ and $M=32$, but for variable constriction length L and the disorder strength W. Shorter constrictions suppress the quantum resonance structure in the WNW geometry.

In Fig. 4 we show the effect of adiabaticity by considering five different structures with the α parameter, which defines adiabaticity, varying as $\alpha=0$ (WNW), 0.25 and 0.50 (rounded), 1.0 (triangular), and ∞ (strip) denoting progressively more adiabatic structures as α increases. We keep all the other system parameters fixed: $W=T=0$, $M=32$, $L=16$, and $M_c=4$. It is clear that the conductance quantization is more accurate for more adiabatic constrictions. However, adiabaticity is, by no means, essential for observing approximate quantization. In the presence of realistic smoothening effects arising from finite temperature and finite (but, small) disorder, even the nonadiabatic WNW structures exhibit reasonably accurate conductance quantization as shown in Figs. 2 and 3.

In Fig. 5 we show the calculated ballistic conductance of two identical WNW constrictions (with fixed $L=4$, $M=16$, and $M_c=4$) in a series. The two constrictions are separated by a distance $D=1$ (a), 2 (b), 3 (c), 4 (d), 5 (e), 6 (f), 7 (g), and 8 (h). It is easy to see that the addition of the law of series resistance is inapplicable to ballistic constrictions, and, in general, for nonadiabatic geometries the conductance quantization is destroyed even at $T=0$ (and for $W=0$) by the quantum resonances arising from two series constrictions. The series resistance is (except for the resonances) of the same order as the individual resistance of each constriction which is believed to be a general result for series ballistic constrictions.

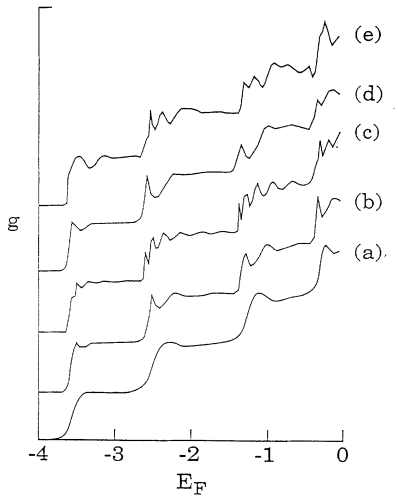

FIG. 3. The $T=0$ conductance in the wide-narrow-wide geometry with $M=32$ and $M_c=4$: (a) $L=4$, $W=0$; (b) $L=9$, $W=0$; (c) $L=16$, $W=0$; (d) $L=8$, $W=0.2$; (e) $L=16$, $W=0.2$.

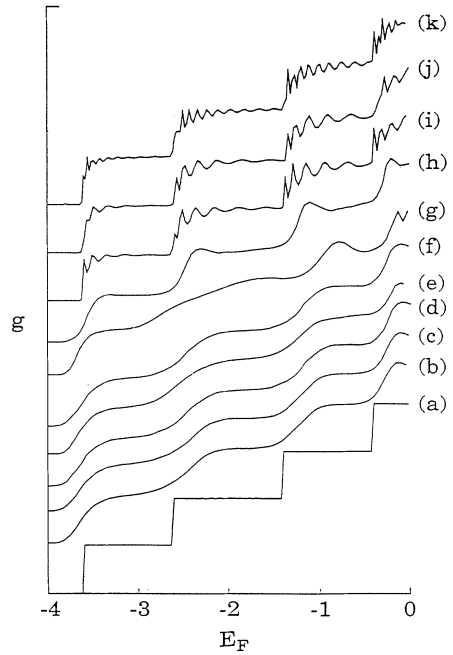

FIG. 4. The $T=0$ and $W=0$ conductance for various constriction geometries defined by the shape parameter α: (a) strip ($\alpha=\infty$); (b) triangular ($\alpha=1$) with $M=16$, $M_c=4$, $L=16$; (c) triangular ($\alpha=1$) with $M=32$, $M_c=4$, $L=16$; (f) parabolic ($\alpha=0.5$) with $M=32$, $M_c=4$, $L=4$; (g) rounded quartic ($\alpha=0.25$) with $M=16$, $M_c=4$, $L=16$; (h) wide-narrow-wide ($\alpha=0$) with $M=32$, $M_c=4$, $L=4$; (i) WNW ($\alpha=0$) with $M=16$, $M_c=4$, $L=16$; (j) WNW ($\alpha=0$) with $M=32$, $M_c=4$, $L=16$; (k) WNW ($\alpha=0$) with $M=32$, $M_c=4$, $L=32$.

Finally, in Fig. 6 we show the effect of a finite external magnetic field on the conductance quantization in the strip and the WNW geometry. In general, a strong magnetic field suppresses the conductance quantization phenomenon by producing additional quantum interference structure on the conductance plateaus, particularly at low temperature and weak disorder. A weak magnetic field, however, helps conductance quantization, as is obvious from our results. In a very strong magnetic field, substantial magnetic depopulation of subbands occurs and, as can be seen from the results, the conductance plateaus shift down and most of them disappear. Note that the very strong quantum interference structure in our high magnetic field results is artificial and arises from our use of an underlying lattice in our calculation.

In comparing our numerical results for the calculated

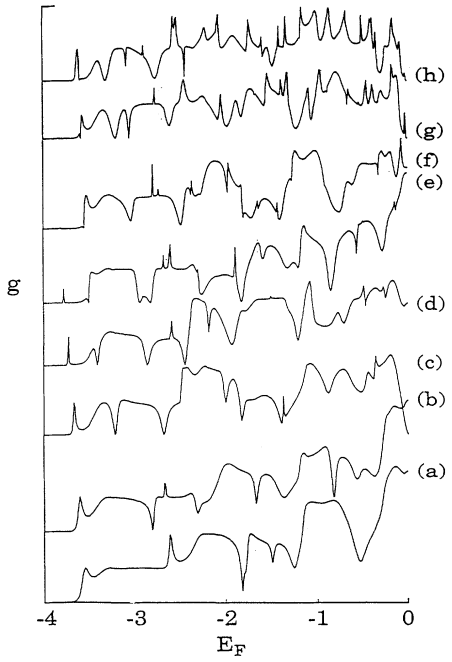

FIG. 5. The conductance of a quasi-one-dimensional structure in the wide-narrow-wide geometry with two identical gates in series. The widths of the wide and narrow regions are $M=16$ and $M_c=4$, respectively. The separation (D) between the two closer edges of the two gates is $D=1$ (a), $D=2$ (b), $D=3$ (c), $D=4$ (d), $D=5$ (e), $D=6$ (f), $D=7$ (g), and $D=8$ (h).

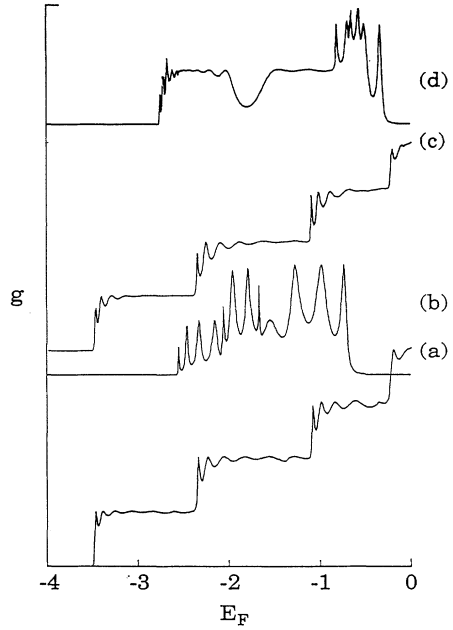

FIG. 6. The effect of an external magnetic field on conductance. In (a) and (b) the constrictions are in the strip geometry with the constriction length $L=16$, and the constriction width $M=4$. The magnetic field is such that the magnetic flux per lattice cell is $\phi=0.0625$ and 0.25 flux quanta in (a) and (b), respectively. In (c) and (d) the constrictions are in the wide-narrow-wide geometry with the width of the wide and narrow region being $M=32$ and $M_c=4$, respectively. The length of the narrow region is $L=16$. The magnetic field is such that the magnetic flux per lattice cell is $\phi=0.0625$ and 0.25 flux quanta in (c) and (d), respectively.

conductance with experimental results[1-3,8] we can only make broad qualitative remarks because the model constrictions are, at best, rather poor imitations of real samples. In fact, the actual geometry of experimental constrictions is, in general, unknown because the constrictions in real samples are produced by electrostatic confinement arising from nanolithographic gates which are typically a few hundred angstroms away from the high-mobility two-dimensional electron gas. While the geometry of the gate structure which produces the confinement is well known, the constriction itself is expected to have a softer edge than the gate and simple models of the type used in this paper are not strictly applicable. There is a related problem in making a direct comparison with the experimental results—experimentally the conductance quantization is observed by tuning the gate voltage which produces a change in the width of the constriction, resulting in a sweep of the chemical potential through the subbands. Theoretically, it is natural to change the chemical potential (as we do in all our presented results) for a geometrically fixed sample and study g as E_F moves through the quantized subbands. It is, in fact, thoroughly nontrivial to accurately model the experimental situation of the tuning of the gate voltage, because both the shape and the size of the constriction as well as the Fermi level change when the gate voltage is tuned. For qualitative discussions aiming at a physical understanding of the conductance quantization phenomenon, it should, however, suffice to obtain g as a function of E_F for fixed constriction geometries, as we do in this paper.

A crucial element which has been much discussed in the literature on the conductance quantization phenomenon is the role played by the adiabaticity of the constrictions. It is clear that in adiabatic constrictions (with low disorder), mode mixing is minimal and the condition $t_{ij}\sim\delta_{ij}$ needed for the conductance quantization phenomenon is well satisfied. Increasing disorder (or, equivalently, increasing the constriction length for a fixed disorder), however, destroys the quantization even in perfectly adiabatic strip geometries. Finite temperature effects in perfectly adiabatic geometries lead to a smoothening of the sharp quantization of each plateau with the jump from one plateau to the next developing a finite slope (rather than being vertically sharp steps). Both finite disorder and finite temperature effects in experimental situations[8] are qualitatively very similar to our numerical results, showing that our simple model calculations catch the essential qualitative physics quite well.

It is indeed true that at $T=0$ (or at very low temperatures, in general), abrupt nonadiabatic constriction (as opposed to an adiabatic constriction) shows poor conductance quantization because of the quantum resonance

structure associated with reflections from sharp corners of the abrupt geometry being superposed on the conductance plateaus. It is clear, however, that with increasing temperature (and, particularly, in the presence of finite disorder) there is virtually no qualitative difference between the abrupt and the adiabatic geometries. We, therefore, conclude that in real samples (i.e., small, but finite W) and at finite (but low) temperatures, the quality of conductance quantization (within 1–2 %) is about the same for both abrupt (WNW) and adiabatic (strip) geometries. The main difference between the abrupt and the adiabatic geometries arises with the lowering of temperature—the quality of conductance quantization should continue to increase with the plateaus becoming sharper in the adiabatic situation and the quantum resonance structure should show up in the abrupt geometry at low temperatures. Thus, the behavior of the temperature dependence of conductance quantization should be sample dependent with adiabatic samples showing better quantization at the lowest temperatures and abrupt structures should have an optimum temperature below which the quantization degrades due to quantum resonances. Again, this behavior is qualitatively consistent[8] with experimental findings. Note that the situation is not as simple as above because of the presence of finite disorder in the sample, which also manifests itself through (irregular) quantum interference structure on the conductance plateaus. At higher temperatures the disorder-induced structure is thermally smoothened out, but even in the perfectly adiabatic strip geometry the low-temperature conductance is not well quantized due to the effect of disorder. Thus, finite (but not too high) temperatures are essential for observing quantized conductance both in abrupt and adiabatic geometries because of the presence of disorder in real systems.

The effect of adiabaticity shown in Fig. 4 indicates that the $T=0$ (and $W=0$) results for a tapered constriction are very similar to finite temperature results in a WNW sample. Thus, finite temperatures and soft rounded constriction boundaries both serve to suppress the quantum resonances. We believe that the real constrictions most likely have α values somewhere around unity, which is intermediate between the extremely abrupt ($\alpha=0$) WNW geometry and the extremely adiabatic ($\alpha=\infty$) strip geometry.

Our approximation scheme for calculating the dimensionless conductance $g \sim \mathrm{Tr}(tt^{\dagger})$ has been a tight-binding lattice Anderson model with on-site random energies simulating elastic disorder in the system. We emphasize that our model incorporates only short-range on-site random disorder whereas real impurity disorder in GaAs microstructures may very well be dominated by long-range Coulomb scatterers. The fact that the low-temperature inelastic mean free path in high-quality GaAs microstructures is very ($\sim$ many micrometers) long[9] makes neglect of realistic inelastic scattering in our calculations a less severe approximation than it may appear at first. (Inclusion of realistic inelastic scattering in the theory in a consistent approximation is a formidable task which has not really been attempted in the literature.) Finally, the modeling of constriction geometry via the on-site diagonal term in the Hamiltonian (by making it very large in regions inaccessible to the electrons so that the electron wave function is vanishingly small outside the specified geometry of the constriction) is an essential approximation of our theory, which, for the level of qualitative understanding we are interested in, is probably adequate. While there is an obvious problem in a quantitative comparison between our model calculations and the experimental results (a continuum description is more appropriate for the real systems), we believe that the qualitative validity of our model is very good.

This work was supported by the U.S.-ONR, the U.S.-ARO, and the Materials Theory (DMR) program of the NSF.

*Present address: AT&T Bell Laboratories, Murray Hill, NJ 07974.

[1]B. J. van Wees, H. van Houten, C. W. J. Beenakker, J. G. Williamson, L. P. Kouwenhoven, D. van der Marel, and C. T. Foxon, Phys. Rev. Lett. **60**, 848 (1988).

[2]D. A. Wharam, T. J. Thornton, R. Newbury, M. Pepper, H. Ahmed, J. E. F. Frost, D. G. Hasko, D. C. Peacock, D. A. Ritchie, and G. A. C. Jones, J. Phys. C **21**, L209 (1988).

[3]H. van Houten, C. W. J. Beenakker, and B. J. van Wees, in *Semiconductors and Semimetals,* edited by M. A. Reed (Academic, New York, 1991), and references therein; C. W. J. Beenakker and H. van Houten, in *Solid State Physics, Advances in Research and Its Applications,* edited by H. Ehrenreich and D. Turnbull (Academic, New York, 1991), Vol. 44, and references therein.

[4]E. N. Economou and C. M. Soukoulis, Phys. Rev. Lett. **46**, 618 (1981); D. S. Fisher and P. A. Lee, Phys. Rev. B **23**, 6851 (1981); P. A. Lee and D. S. Fisher, Phys. Rev. Lett. **47**, 882 (1981).

[5]G. Kirczenow, Solid State Commun. **68**, 715 (1988); A. Szafer and A. D. Stone, Phys. Rev. Lett. **62**, 300 (1989); E. G. Haanappel and D. van der Marel, Phys. Rev. B **39**, 5484 (1989); L. Escapa and N. Garcia, J. Phys. Condens. Matter **1**, 2125 (1989); Y. Avishai and Y. B. Band, Phys. Rev. B **41**, 3253 (1990); L. I. Glazman and M. Johnson, *ibid.* **41**, 10 686 (1991); A. Kumar and P. F. Bagwell, *ibid.* **44**, 1747 (1991); E. Tekman and S. Ciraci, *ibid.* **43**, 7145 (1991); T. Ando, *ibid.* **44**, 8017 (1991).

[6]Song He and S. Das Sarma, Phys. Rev. B **40**, 3379 (1989); Solid State Electron. **32**, 1695 (1989).

[7]P. A. Lee, A. D. Stone, and H. Fukuyama, Phys. Rev. B **35**, 1039 (1987); X. C. Xie and S. Das Sarma, *ibid.* **38**, 3529 (1988).

[8]B. J. van Wees, L. P. Kouwenhoven, H. van Houten, C. W. J. Beenakker, J. E. Mooij, C. T. Foxon, and J. J. Harris, Phys. Rev. B **38**, 3625 (1988); Y. Hirayama, T. Saku, and Y. Horikoshi, *ibid.* **39**, 5535 (1989); Y. Hirayama and T. Saku, *ibid.* **41**, 2927 (1990); J. Faist, P. Guéret, and H. Rothuizen, *ibid.* **42**, 3217 (1990); D. A. Wharam, M. Pepper, H. Ahmed, J. E. F. Frost, D. G. Hasko, D. C. Peacock, D. A. Ritchie, and G.

A. C. Jones, J. Phys. C **22**, L887 (1988); Y. Hirayama and T. Saku, Appl. Phys. Lett. **54**, 2556 (1989); G. Timp, R. E. Behringer, and J. E. Cunningham, Phys. Rev. B **42**, 9259 (1990); B. J. van Wees, L. P. Kouwenhoven, E. M. M. Willems, C. J. P. M. Harmans, J. E. Mooij, H. van Houten, C. W. J. Beenakker, J. G. Williamson, and C. T. Foxon, *ibid.* **43**, 12 431 (1991).

[9]R. Jalabert and S. Das Sarma, Phys. Rev. B **40**, 9723 (1989); Solid State Electron. **32**, 1259 (1989).